IMPLEMENTATION OF A NEURO FUZZY CONTROL STRATEGY FOR OPTIMIZING THE ENERGY PERFORMANCE OF A HYBRID AIR BASED PVT COLLECTOR. APPLICATION TO THE MAHAJANGA SITE

TSARAZAKA Yves Germain[1], HANITRANIRINA Eloddy[1], TOVONDRAINY Ramiandrisoa[1], RAHARIJAONA Petera[1], DONA Victorien Bruno[2]

[1]PhD Student, Laboratory of Applied Physics and Renewable Energies (LPAER), Doctoral School of Life Sciences and Modeling (EDGVM), University of Mahajanga, Madagascar
[2]Professor, Laboratory of Applied Physics and Renewable Energies (LPAER), Doctoral School of Life Sciences and Modeling (EDGVM), University of Mahajanga, Madagascar

ABSTRACT

The Mahajanga region benefits from exceptional solar resources, characterized by one of the highest levels of solar irradiation in Madagascar, thus providing optimal conditions for the operation of photovoltaic generators. Air-based hybrid photovoltaic-thermal (PVT) systems demonstrate superior energy efficiency due to their cogeneration capability. This study presents an original neuro-fuzzy MPPT control approach applied to air-based PVT systems within the specific context of Mahajanga. The results indicate a marked improvement in tracking accuracy compared to conventional methods, offering concrete prospects for energy optimization in tropical regions. The system processes the measured electrical parameters in real time, utilizing the instantaneous error (E) and its variation (ΔE) to determine the optimal duty cycle (D) of the Boost converter. The comparative analysis with the conventional P&O algorithm demonstrates a significant improvement in energy performance through the neuro-fuzzy approach, validating its potential for optimizing the exploitation of Mahajanga's solar resources.

Keywords: Air-based PVT, Artificial Intelligence, Neuro-fuzzy system, MPPT, performance, Optimization, Renewable energies, Mahajanga.

1. INTRODUCTION

The Mahajanga region benefits from exceptional solar resources, characterized by some of the highest levels of solar irradiation in Madagascar. This abundant solar resource offers ideal conditions for the deployment of photovoltaic (PV) generators, the technical and economic feasibility of which is well established. However, for optimal valorization of this abundant resource, hybrid photovoltaic-thermal (PVT) air generators represent a promising innovation. Their main advantage lies in their cogeneration capability, allowing simultaneous electricity production through the photovoltaic effect and thermal energy recovery via an air flow circulating beneath the modules. This energy synergy not only improves electrical efficiency by cooling the PV cells but also provides hot air for various applications, thus optimizing the overall system efficiency.

Optimizing the performance of these systems relies essentially on the efficiency of Maximum Power Point Tracking (MPPT) algorithms. Among the different existing MPPT approaches, we mainly distinguish conventional methods [1] such as Perturb and Observe (P&O) and Incremental Conductance, intelligent techniques including Artificial Neural Networks (ANN) and fuzzy logic, as well as hybrid approaches like neuro-fuzzy systems [3].

In this context, this study proposes the implementation of an innovative neuro-fuzzy (ANFIS) MPPT control system to optimize the performance of air-based PVT generators. The neuro-fuzzy system uses as input variables the instantaneous error (E) and its variation (ΔE), calculated from real-time current and voltage measurements. These parameters allow the controller to accurately determine the optimal duty cycle (D) of the Boost converter. The comparative performance analysis with the conventional P&O algorithm demonstrates the superiority of the neuro-fuzzy (ANFIS) approach for fully exploiting Mahajanga's exceptional solar potential, thereby validating its superior energy efficiency.

2. METHODOLOGY

2.1 System Configuration

The air-based PVT MPPT-ANFIS system, illustrated in Fig-1, consists of a hybrid photovoltaic-thermal (PVT) air generator, connected to a Boost converter and controlled by an ANFIS controller.

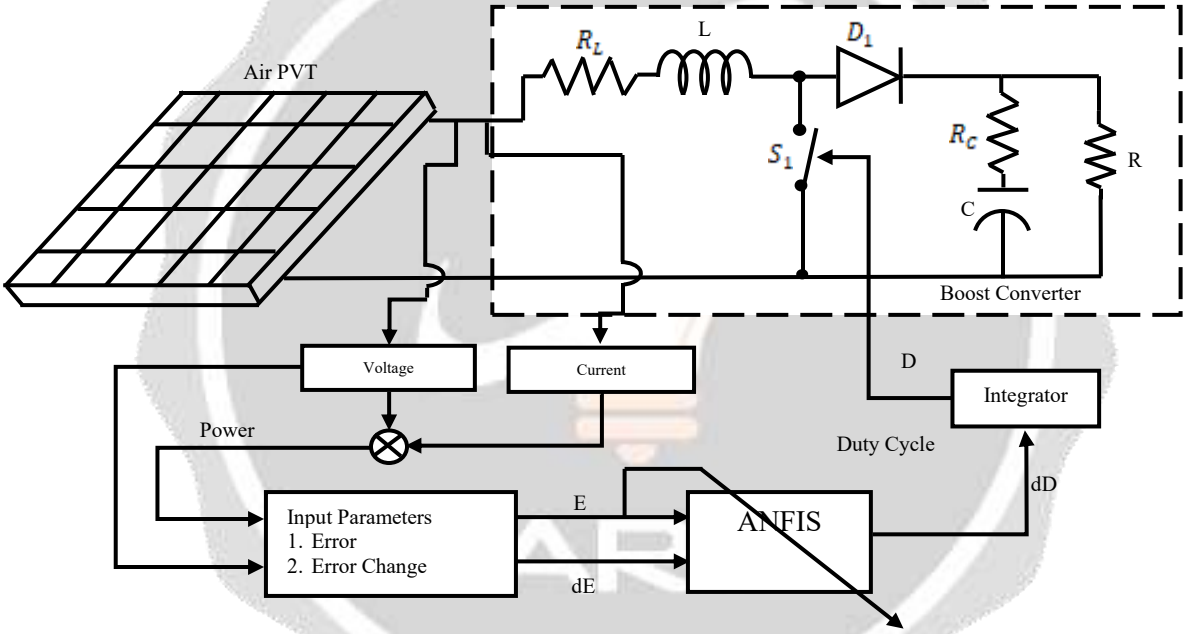

Fig -1: Configuration of the air-based PVT MPPT-ANFIS system [2]

2.2 Operating Principle

The air-based PVT MPPT-ANFIS system relies on a neuro-fuzzy (ANFIS) MPPT control structured in five layers and using 25 fuzzy rules. The process begins with the real-time acquisition of the electrical parameters (voltage and current) of the PVT generator, allowing the calculation of the error (E) and its variation (ΔE). These parameters are normalized and then processed by the neuro-fuzzy architecture. The ANFIS system generates as output a variation of the duty cycle (dD) which adjusts the DC-DC Boost converter. This intelligent control optimizes in real-time the operating point to reach the optimal values of voltage (V_{ppm}) and current (I_{ppm}), ensuring maximum power production regardless of weather conditions. Simulations demonstrate the superiority of this approach compared to traditional MPPT methods [1,19], with reduced oscillations, accelerated convergence, and improved energy efficiency. These performances are achieved thanks to the synergy between the learning capability of neural networks and the flexibility of fuzzy reasoning to handle uncertainties.

2.3 Modeling of the Hybrid Air-based PVT Collector

The hybrid air-based PVT collector adopted in this study is inspired by the model developed by TOUAFEK Khaled [5]. This multi-layer configuration optimizes energy conversion through a design integrating both photovoltaic electricity production and thermal recovery.

2.3.1 Simplifying Assumptions

Before establishing the energy balance equations for each component, the following assumptions were adopted [4,5,8,11] :

- The ground temperature is taken equal to the ambient temperature.
- The physical properties of the materials are assumed constant.
- The wind is assumed to be blowing parallel to the system faces.
- Atmospheric diffuse radiation is isotropic.
- The flow regime is transient.
- The EVA transmission coefficient is 100%.

2.3.2 Model Descriptions

The hybrid air-based PVT collector adopted in this study is inspired by the model developed by TOUAFEK Khaled [5]. This configuration allows both photovoltaic conversion and thermal energy recovery by convection with the circulating air flow.

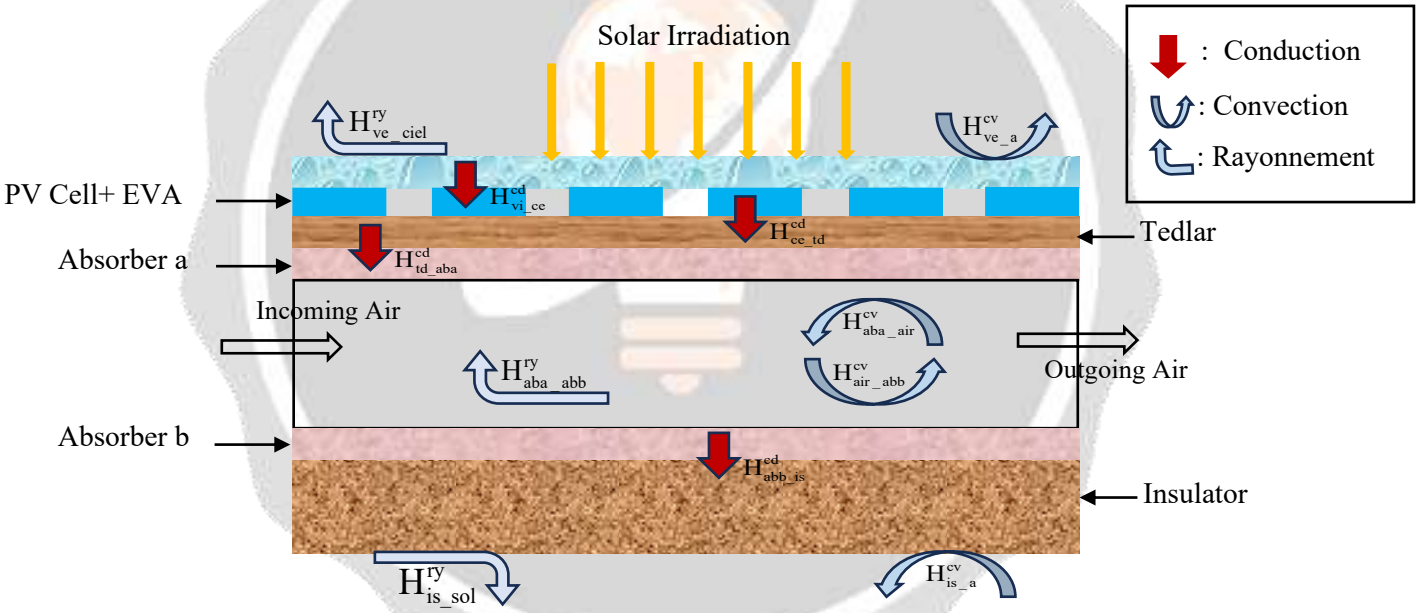

Fig -2: Hybrid air-based PVT collector proposed by TOUAFEK Khaled [5]

2.3.3 Equivalent Electrical Circuit

To model the thermal transfers, the physical structure of the air-based PVT collector is transposed into an equivalent electrical circuit (Fig-3) [6]. This electro-thermal analogy allows representing the heat exchanges between the different layers of the system. The model considers the thermal resistances and heat capacities of each component, thus facilitating the analysis of the overall energy performance of the collector.

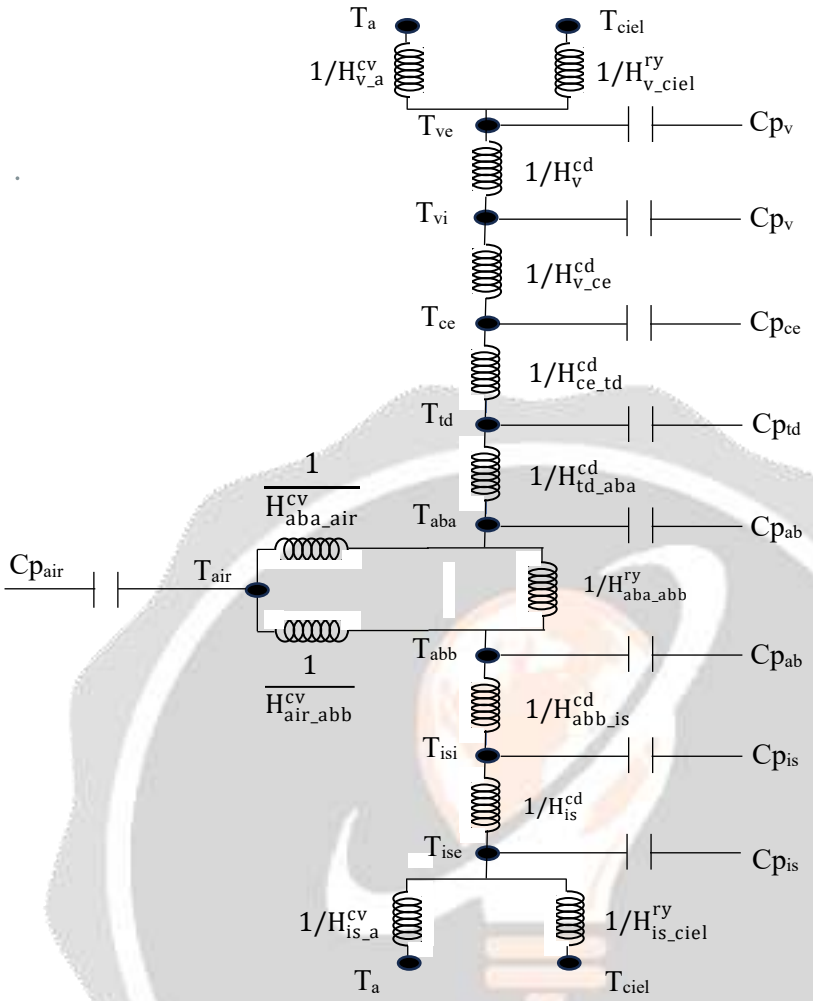

Fig -3: Equivalent electrical circuit of thermal transfers in the air-based PVT [6,7]

Based on this electro-thermal analogy, the energy balances at the different nodes are expressed by: [5,11]

Node1: External face of the glass

$$\frac{M_v Cp_v}{S_v}\left(\frac{dT_{ve}}{dt}\right) = G_i - H^{cv}_{ve\_a}\left(T_{ve} - T_a\right) - H^{cd}_{v}\left(T_{ve} - T_{vi}\right) - H^{ry}_{ve\_ciel}\left(T_{ve} - T_{ciel}\right) \quad (1)$$

Node2: Internal face of the glass

$$\frac{M_v Cp_v}{S_v}\left(\frac{dT_{vi}}{dt}\right) = \alpha_v . G_i + H^{cd}_{v}\left(T_{ve} - T_{vi}\right) - H^{cd}_{vi\_ce}\left(T_{vi} - T_{ce}\right) \quad (2)$$

Node 3: PV cell

$$\frac{M_{ce} Cp_{ce}}{S_{ce}}\left(\frac{dT_{ce}}{dt}\right) = \tau_v . \alpha_v . G_i + H^{cd}_{vi\_ce}\left(T_{vi} - T_{ce}\right) - H^{cd}_{ce\_td}\left(T_{td} - T_{ce}\right) - P_{élec} \quad (3)$$

Node4: Tedlar

$$\frac{M_{td} Cp_{td}}{S_{td}}\left(\frac{dT_{td}}{dt}\right) = H^{cd}_{ce\_td}\left(T_{ce} - T_{td}\right) - H^{cd}_{td\_aba}\left(T_{td} - T_{aba}\right) \quad (4)$$

Node5: Absorber

$$\frac{M_{ab}Cp_{ab}}{S_{ab}}\left(\frac{dT_{aba}}{dt}\right)=H^{cd}_{td\_aba}\left(T_{td}-T_{aba}\right)-H^{cv}_{aba\_air}\left(T_{aba}-T_{air}\right)-H^{ry}_{aba\_abb}\left(T^4_{aba}-T^4_{abb}\right) \quad (5)$$

Node6: Fluid

$$\frac{M_{air}Cp_{air}}{S_{air}}\left(\frac{dT_{air}}{dt}\right)=H^{cv}_{aba\_air}\left(T_{aba}-T_{air}\right)+H^{cv}_{air\_abb}\left(T_{air}-T_{abb}\right)-\dot{m}\,Cp_{air}\left(T_{air\_sort}-T_{air\_entr}\right) \quad (6)$$

Node7: Absorber B

$$\frac{M_{ab}Cp_{ab}}{S_{ab}}\left(\frac{dT_{abb}}{dt}\right)=H^{cv}_{air\_abb}\left(T_{air}-T_{abb}\right)-H^{cd}_{abb\_is}\left(T_{abb}-T_{isi}\right)+H^{ry}_{aba\_abb}\left(T^4_{aba}-T^4_{abb}\right) \quad (7)$$

Node 8: Internal face of the insulator

$$\frac{M_{is}Cp_{is}}{S_{is}}\left(\frac{dT_{isi}}{dt}\right)=H^{cd}_{abb\_is}\left(T_{abb}-T_{isi}\right)-H^{cd}_{is}\left(T_{isi}-T_{ise}\right) \quad (8)$$

Node 9: External face of the insulator

$$\frac{M_{is}Cp_{is}}{S_{is}}\left(\frac{dT_{ise}}{dt}\right)=H^{cd}_{is}\left(T_{isi}-T_{ise}\right)-H^{cv}_{is\_a}\left(T_{ise}-T_a\right)-H^{ry}_{is\_sol}\left(T_{ise}-T_{sol}\right) \quad (9)$$

Node 9: External face of the insulator

$$\frac{M_{is}Cp_{is}}{S_{is}}\left(\frac{dT_{ise}}{dt}\right)=H^{cd}_{is}\left(T_{isi}-T_{ise}\right)-H^{cv}_{is\_a}\left(T_{ise}-T_a\right)-H^{ry}_{is\_sol}\left(T_{ise}-T_{sol}\right) \quad (10)$$

These equations are solved numerically by the iterative Gauss-Seidel method [4,8], allowing accurate determination of the thermal distribution across all layers of the PVT collector.

2.3.4 Electrical Model of the Hybrid Air-based PVT Collector

The photovoltaic panel electrical model retained for the hybrid air-based PVT collector is based on the single-diode approach. The electrical behavior of the system is determined from a set of electrical parameters whose values closely depend on solar irradiation (G) and cell temperature (T_{pvt}) [9,20]. The configuration adopted in our modeling features N_s = 42 cells in series and N_p = 1 parallel branch. This specific configuration determines the output electrical characteristics according to the relationships:

$$\begin{cases} I_{pv}=N_p.I_{ph}-N_p.I_o\left[\exp\left(q\dfrac{V_{pv}+I_{pv}.R_s}{n.N_s.K.T}\right)-1\right]-\dfrac{V_{pv}+I_{pv}.R_s}{R_{sh}} \\ I(G,T_{pv})=I_{ref}+\Delta I=I_{ref}+k_i\left(\dfrac{G}{G_{ref}}\right)\Delta T+\left(\dfrac{G}{G_{ref}}-1\right)I_{sc,ref} \\ V(G,T_{pvt})=V_{ref}+\Delta V=V_{ref}+k_V.\Delta T-R_s.\Delta I \\ I_{sc}\left(G,T_{pvt}\right)=\left(\dfrac{G}{G_{ref}}\right)\left(k_i.\Delta T+I_{sc,ref}\right) \\ V_{oc}\left(G,T_{pv}\right)=V_{oc,ref}+k_V.\Delta T+n\ln\left(\dfrac{G}{G_{ref}}\right) \\ \Delta T=T_{pv}-T_{pv,ref} \end{cases} \quad (11)$$

2.3.5 Hybrid Collector Performance

Maximum Power Pv

The maximum power of an illuminated cell Pv is the essential quantity to evaluate its performance ; it is given by the relation [10] :

$$P_m = V_m \times I_m \tag{12}$$

Puissance électrique PVT

PVT Electrical Power

The electrical power (Pelec) produced by the air-based PVT panels is calculated from the irradiance on the collector plane G, the total surface area of the photovoltaic cells, and the electrical efficiency [6,7].

$$\begin{cases} P_{elec} = \eta_{elec} \times S_{cel} \times G \\ \eta_{elec} = \eta_{ref} \times \left[1 - 0.0045\left(T_{ce} - T_{ref}\right)\right] \end{cases} \tag{13}$$

Thermal Efficiency of the PVT Collector

The thermal efficiency is the determining factor of its thermal performance, which is determined by the following formula [11] :

$$\eta_{th} = \frac{P_{th}}{S_{cel}.G} = \frac{\dot{m}_f \, Cp_f \left(T_{fs} - T_{fe}\right)}{S_{cel}.G} \tag{14}$$

Electrical Efficiency of a PVT Collector

The solar cell efficiency depends on the cell temperature and is given by [12]:

$$\eta_{elec} = \eta_{ref}\left[1 - \beta\left(T_{pv} - T_{ref}\right)\right] \tag{15}$$

Overall Efficiency of the PVT Collector

The overall efficiency of the photovoltaic-thermal collector is defined as the sum of the electrical efficiency and the equivalent thermal efficiency [13,18]

$$\begin{cases} \eta_{global} = \eta_{th} + \eta_{elec,th} \\ \eta_{elec,th} = \dfrac{\eta_{elec}}{C_f} \end{cases} \tag{16}$$

2.4 Neuro-Fuzzy Control for the PVT hybrid air collector.

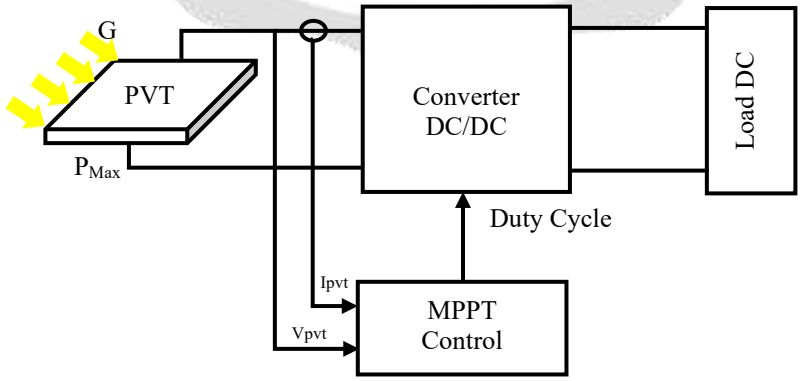

Fig -4: Schematic of a PVT system with MPPT control. [2]

Fig-4 presents the general architecture of a PVT system integrating MPPT control. The MPPT (Maximum Power Point Tracker) device, associated with a DC-DC converter [2], ensures the permanent operation of the photovoltaic generator at its maximum power point. The control strategy acts on the converter's duty cycle automatically, maintaining the system at the optimal operating point despite variations in weather conditions or sudden load changes.

2.4.1 ANFIS Architecture

ANFIS (Adaptive Neuro-Fuzzy Inference System) uses a Takagi-Sugeno type Fuzzy Inference System (FIS). Its architecture, represented in Fig-5, consists of five distinct layers [3]. To illustrate its operation, consider a fuzzy inference system with two inputs (x, y) and one output (s). The Takagi-Sugeno type fuzzy system is defined by the following rules [16] :

$$\begin{cases} \text{Rule1: if x is } A_1 \text{ and y is } B_1 \text{ then} & s_1 = p_1 x + q_1 y + r_1 \\ \text{Rule2: if x is } A_2 \text{ and y is } B_2 \text{ then} & s_2 = p_2 x + q_2 y + r_2 \end{cases} \quad (17)$$

A_1, A_2, B_1 et B_2 are fuzzy sets

p_i, q_i, r_i are the consequent parameters of rule i determined during the learning process.

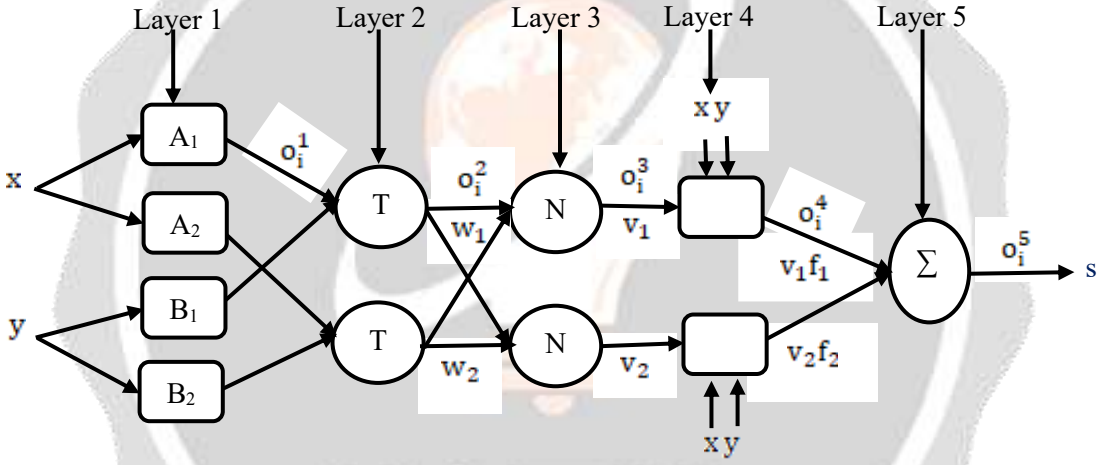

Fig -5: General architecture of ANFIS.[13]

ANFIS is a multilayer neural network without weights (weights = 1) on the connections. Its nodes are classified into two categories according to their function [3]: square nodes (adaptive, with parameters) and circular nodes (fixed, without parameters). Each node executes an operation on its inputs. Thus, the output o_i^k of node i in layer k (called node (i, k)) depends on signals from layer (k-1) and the parameters of node (i, k).

$$o_i^k = f\left(o_i^{k-1}, ..., o_{n_{k-1}}^{k-1}, a, b, c, ...\right) \quad (18)$$

n_{k-1} : number of nodes in layer k-1,

a, b, c: parameters of node (i, k). For a circular node these parameters do not exist.

First layer : Fuzzification

Each node in this layer has adjustable parameters. The function of each node corresponds to a membership function [14], calculating the degree of membership of the inputs to the defined fuzzy sets.

$$o_i^1 = f_i^1(x) = \mu_{Ai}(x) \quad (19)$$

x is input to node i, and A_i the linguistic term associated with its function μ_{Ai}

o_i^1 is the degree of membership of x to A_i defined by the membership function $\mu_{Ai}(x)$

Second layer : Multiplication of inputs with each other
Also called the first hidden layer, it serves to calculate the firing strength of the premises. Each circular node T corresponds to a Sugeno-type fuzzy rule. It takes the outputs from the fuzzification nodes and then calculates its activation.

$$w_i = \mu_{Ai}(x).\mu_{Bi}(y) \qquad \text{Avec } i = 1,2 \tag{20}$$

Third layer : Normalization of the rule weights
Also called the second hidden layer. The circular nodes N calculate the normalized firing strength of a given fuzzy rule.

$$v_i = \frac{w_i}{w_1 + w_2} \tag{21}$$

Fourth layer : Calculation of rule outputs
Called the third hidden layer. The nodes in this layer are square.

$$o_i^4 = v_i.f_i = v_i\left(a_i x + b_i y + c_i\right) \text{ Avec } i = 1,2 \tag{22}$$

v_i is the output of layer 3

$\{a_i, b_i, c_i\}$ is the set of adjustable output parameters of rule i.

Fifth layer or output layer: Summation of all inputs
This layer contains a single node. It provides the output of ANFIS.

2.5 Design of an MPPT Controller Based on a Neuro-Fuzzy Network
This section presents the implementation of an MPPT control based on an ANFIS network [15]. The objective of this intelligent controller is to optimize in real-time the operating point of a photovoltaic system to maximize its energy production. The block diagram in Fig-6 illustrates the integration of this control into the PVT system.

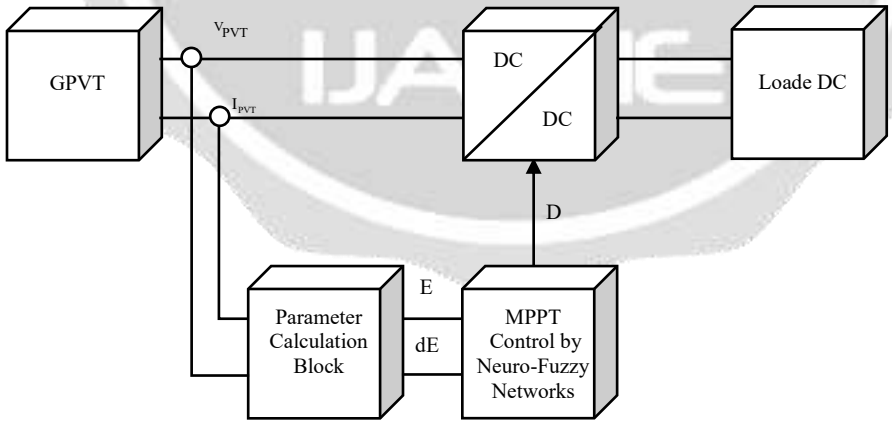

Fig -6: Architecture of the PVT system with MPPT control based on a neuro-fuzzy network.

2.5 Architecture and Principles of the Neuro-Fuzzy MPPT Controller

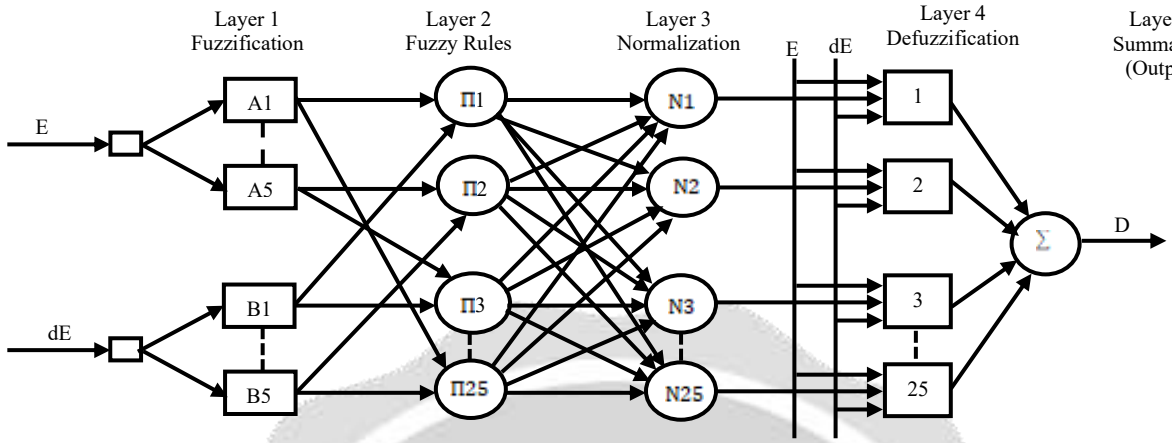

Fig -7: Architecture of the ANFIS model.

The detailed architecture of the ANFIS model is presented in Fig-7. The neuro-fuzzy MPPT controller receives as input the error (E) and its variation (ΔE), and generates as output the command (D). This latter ensures both the prediction and optimization of the duty cycle applied to the DC/DC converter, guaranteeing the dynamic adaptation of the PVT generator's power to the optimal operating point. The system automatically generates its fuzzy rules according to the Sugeno inference model, while neural learning optimizes the precision and robustness of the control [13,15]. The complete algorithm of the MPPT control by neuro-fuzzy network is illustrated in Fig-8 [16], detailing the successive steps of reading, normalization, ANFIS processing, and generation of the optimal command.

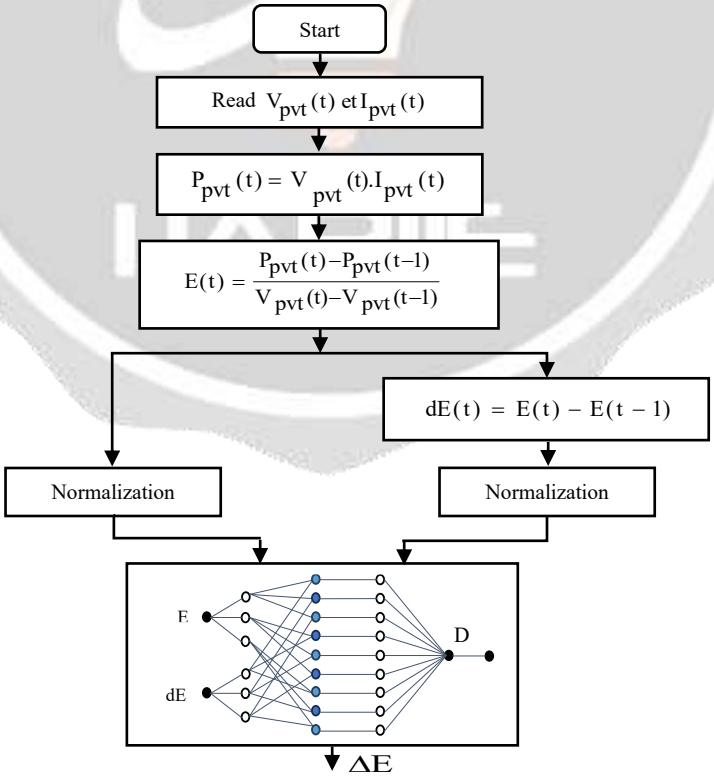

Fig -8: Algorithm of MPPT control by neuro-fuzzy network [16]

3. RESULTS AND DISCUSSIONS

This study focuses on the Mahajanga region, located in northwestern Madagascar (15°43' South, 46°19' East). The meteorological data used come from ASECNA and cover the period 2010-2024. The estimation of global solar irradiation was performed by applying the Page model [21,22], recognized for its accuracy in tropical regions.

3.1 Variation of Global Irradiation and Ambient Temperature

The comparative analysis of global solar irradiation profiles and ambient temperature in Mahajanga reveals superior energy performance in October compared to January. Both parameters reach their peak levels between 12:00 PM (noon) and 14:00, a period corresponding to the most intense thermal flux of the day.

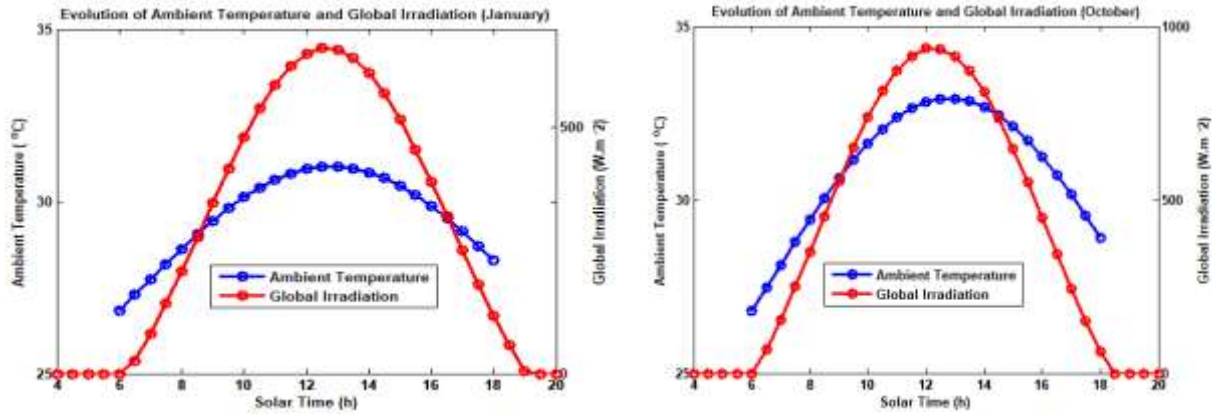

Fig -9: Global irradiation and ambient temperature

3.2 Variation of Electrical Power

The PVT system reaches a maximum electrical power of 173.3 W in October compared to 126.5 W in January, with a daily peak systematically observed between 12 :00 pm and 14 :00, the period of optimal solar radiation. The ANFIS model demonstrates remarkable prediction accuracy, closely following the real data with negligible relative error. This performance validates the effectiveness of the neuro-fuzzy approach for predicting and optimizing the electrical performance of the system.

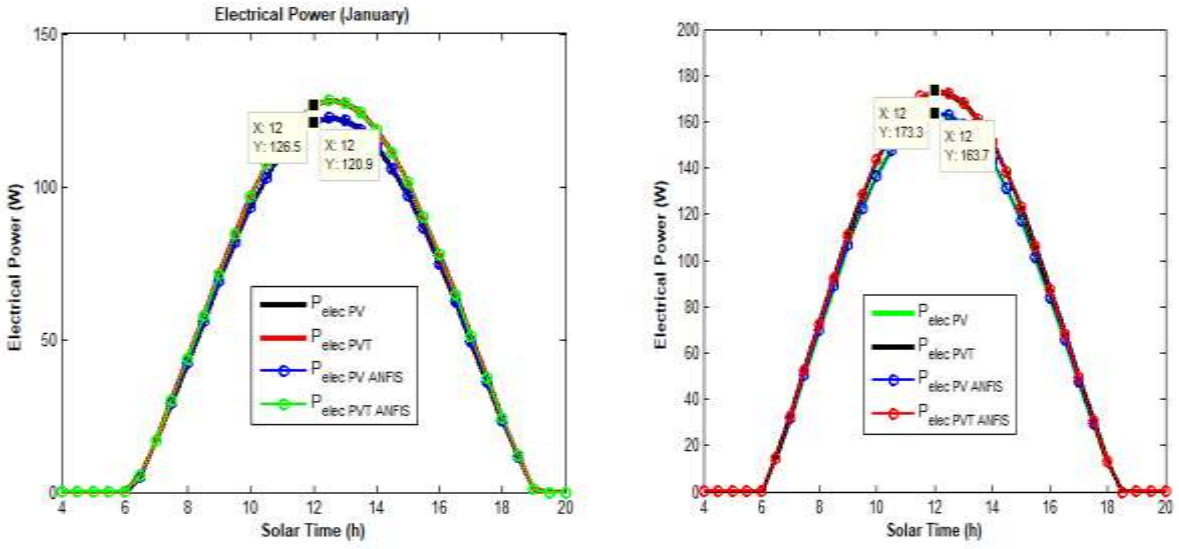

Fig -10: Electrical power of the PVT model and predicted by ANFIS

3.3 Variation of Electrical Efficiency

A comparative analysis of the electrical output between the months of October and January reveals superior performance during the first of these two months. A decrease in performance is observed between 12 :00 pm and 14 :00 in both cases, attributable to the rise in cell temperature during periods of high solar irradiance. The perfect match between the outputs predicted by the ANFIS model and the model's outputs confirms the robustness of the proposed approach.

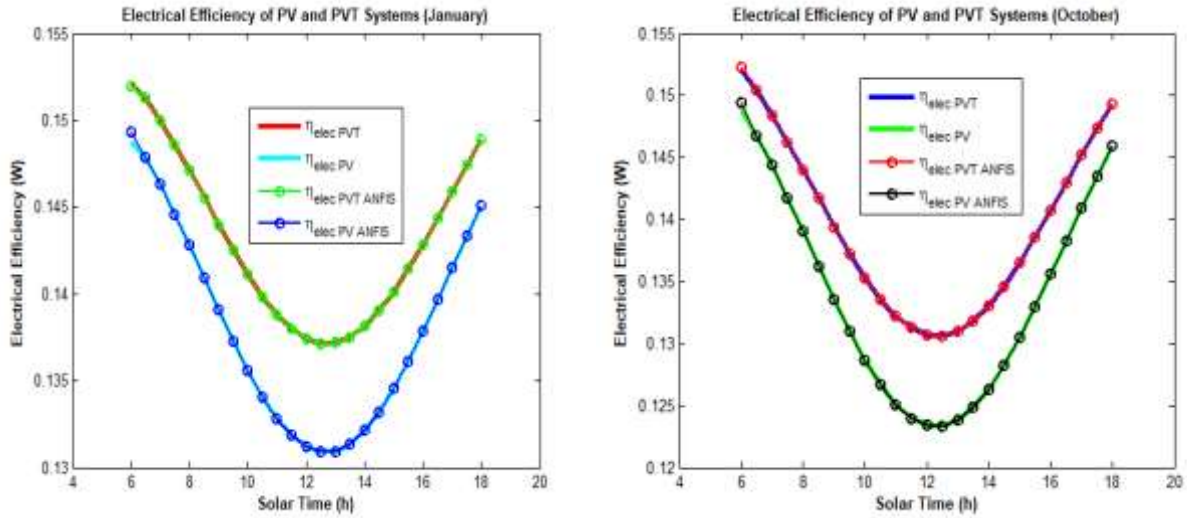

Fig-11: Electrical efficiency of the model and predicted by ANFIS

3.4 Variation of Thermal Efficiency

The thermal efficiency of the PVT system (Fig-12) shows superior performance in October, with a maximum of 58% against 51% in January. Contrary to electrical efficiency, an improvement in thermal performance is observed between 12:00 pm and 14:00, taking advantage of maximum sunlight for increased thermal recovery. The agreement between the predicted and reference curves demonstrates the ability of the ANFIS algorithm to simultaneously model the electrical and thermal components of the hybrid PVT system.

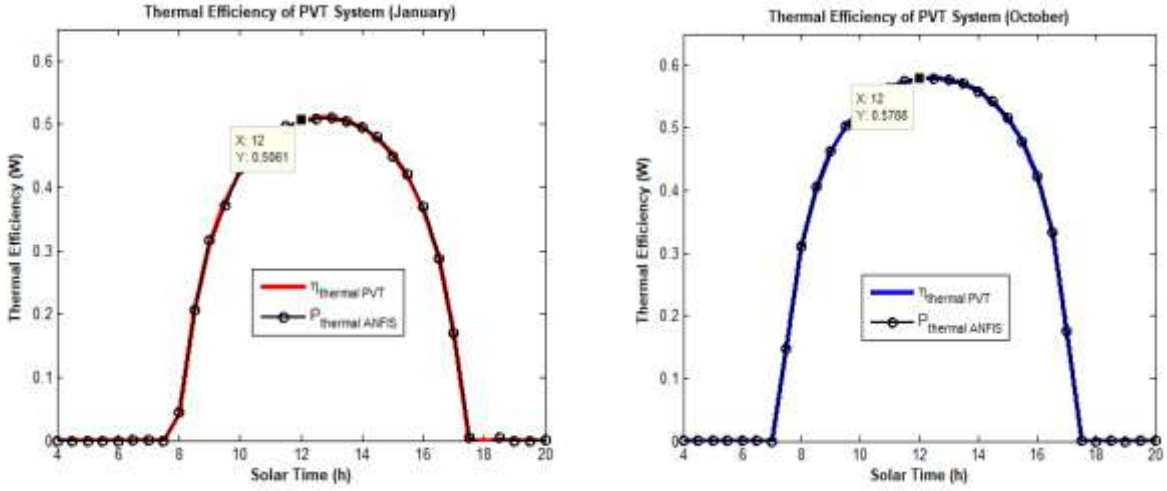

Fig-12: Thermal efficiencies of the model and predicted by ANFIS

3.5 Variation of Overall Efficiency

The comparative evolution of overall efficiency (Figure 13) reveals superior energy performance in October, with a maximum of 91% against 85% in January. This difference is mainly explained by more favorable sunlight conditions in October, allowing optimized simultaneous energy production. The peak efficiency located between 12:00 pm and 14:00 for both months corresponds to the daily maximum solar radiation. These results validate the accuracy of the ANFIS model for predicting overall efficiency under different seasonal conditions.

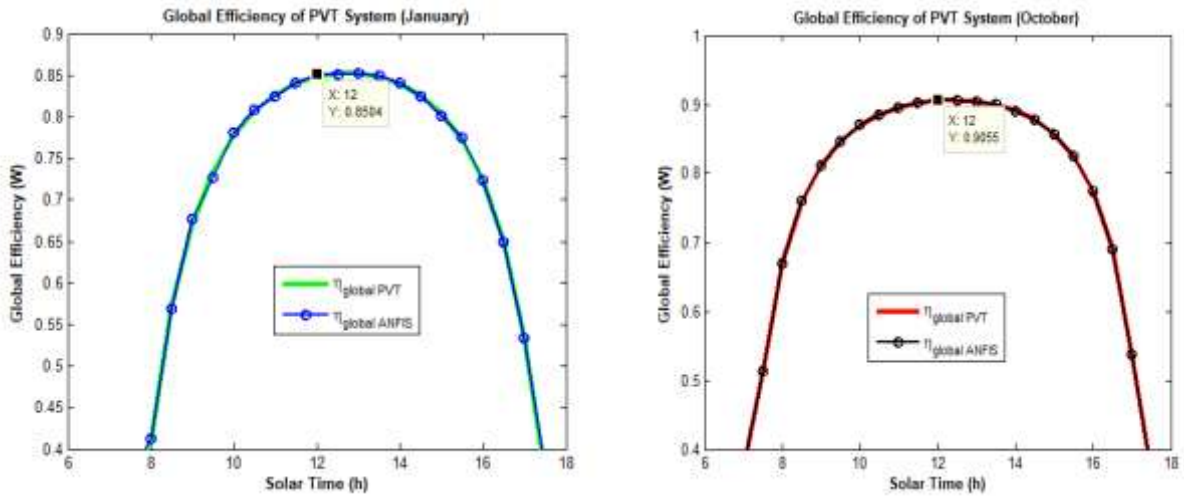

Fig-13: Overall efficiency of the model and predicted by ANFIS

3.6 Characteristic P(V) of PV-PVT System with and without MPPT by P&O and ANFIS

The analysis of the P-V characteristics (Fig-14 and Fig-15) reveals significant differences between the MPPT approaches. Optimization by P&O limits relative errors to 5.63% for PV and 5.14% for PVT, while the neuro-fuzzy approach reduces them to 3.02% and 2.12% respectively. This notable reduction in errors demonstrates ANFIS's ability to faithfully reproduce the behavior of PV/PVT systems while offering superior accuracy to the conventional P&O method.

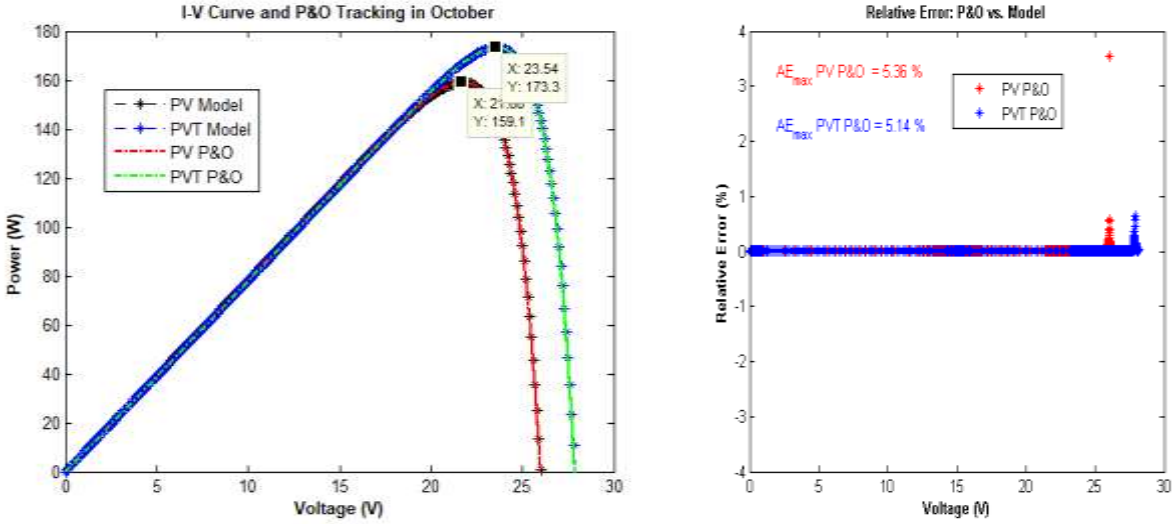

Fig-14: Characteristic (P-V) with and without MPPT by P&O and its relative errors

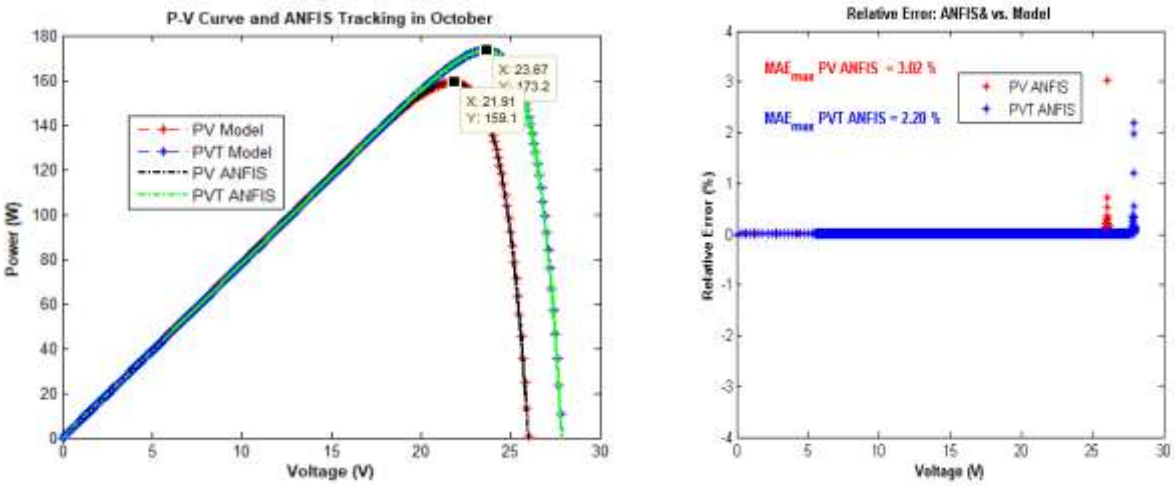

Fig-15: Characteristic (P-V) with and without MPPT by ANFIS and its relative errors

3.7 Characteristics P(V) of PV-PVT system under different irradiations, with MPPT by P&O and ANFIS

The P(V) curves clearly show that the PVT system generates higher power than PV alone at each irradiation level. This improvement is due to thermal cooling which increases electrical efficiency. This result is verified for both MPPT methods used. The P&O MPPT allows the PVT to reach a higher power peak. With the ANFIS MPPT, the PVT maintains this advantage while benefiting from faster and more precise tracking of the maximum power point. Thus, thermal integration in a PVT system improves electrical production. Moreover, the ANFIS algorithm proves more performant than the P&O method to fully exploit this energy potential. The obtained curves are consistent with the experimental study conducted by Bouden Abdelmalek [11].

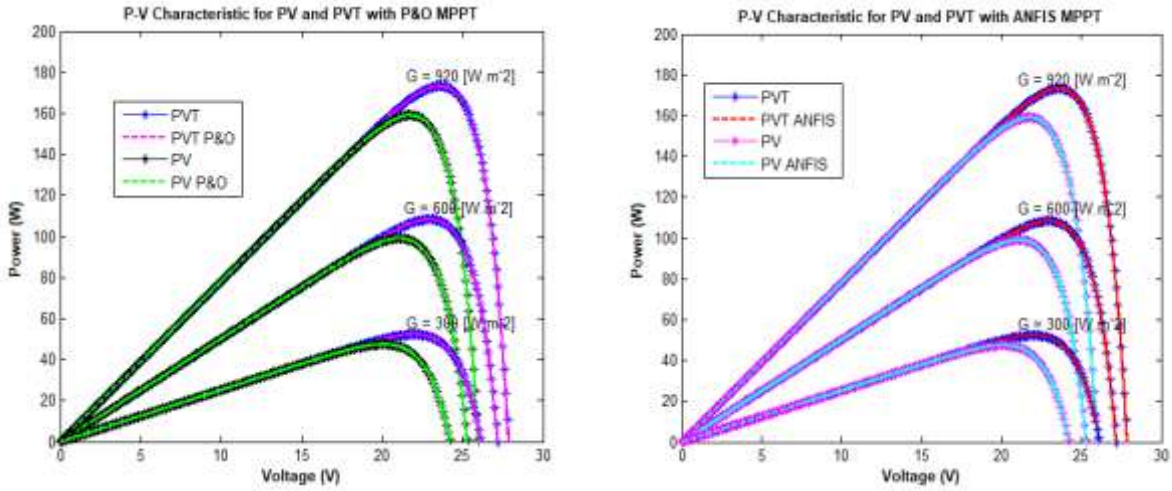

Fig-16: Characteristics P-V of the PV-PVT system under different irradiations, with P&O MPPT and ANFIS MPPT

4. CONCLUSIONS

This study demonstrates the superiority of the ANFIS neuro-fuzzy system for MPPT control of air-based photovoltaic-thermal systems. The analysis of the P-V curves (Fig. 14-16) reveals that ANFIS effectively eliminates oscillations around the maximum power point observed with the P&O method, while ensuring more precise and faster tracking under variable irradiation conditions. Compared to the conventional P&O method, the ANFIS approach presents significant advantages in terms of precision, stability, and adaptability.

The experimental results confirm that ANFIS reduces relative errors to 3.02% for PV systems and 2.20% for PVT systems, compared to 5.36% and 5.14% respectively for the P&O method. The strong correlation between ANFIS predictions and real measurements validates its dynamic adaptation capabilities and robustness in the face of

environmental variations. These conclusions support the adoption of neuro-fuzzy methods for optimizing hybrid energy systems and open promising perspectives for the large-scale deployment of renewable energies in the Mahajanga region.

4. REFERENCES

[1]. Bouden Abdelmalek, 'Modélisation numérique de nouveaux systèmes à ENR Application au Pompage', thèse de doctorat, Université des Frères Mentouri Constantine Faculté des Sciences de la Technologie département d'électronique, 08/11/2018

[2] F.Belhachat, C. Larbes, L. Barazane, S. Kharzi ,'Commande neuro-floue d'un hacheur MPPT', Article, 4th International Conference on Computer Integrated Manufacturing CIP' 2007, 03-04 November 2007

[3] BACHIRI Lakhdar MIDA Ammar, 'Étude d'un système photovoltaïque optimisé par une technique MPPT intelligente (neurone-floue) ANFIS', Mémoire Master, Universite Kasdi Merbah Ouargla Faculté des Sciences Appliquées Département de Génie Electrique, 2020/2021

[4]. Roula Badreddine et Boulouaret Hocine.' L'influence des paramètres de fonctionnement Sur les performances d'un capteur hybride PVT', Mémoire de master, Université Mohamed Seddik Ben Yahia - Jijel, Soutenue 26 /10/2020.

[5]. TOUAFEK Khaled.' Contribution à l'étude et à la conception d'un système énergétique utilisant des capteurs hybrides photovoltaïques thermiques, thèse de doctorat, École nationale polytechnique, Département d'électronique, Algérienne, 2010.

[6]. Oussama El Manssouri, Bekkay Hajji, Giuseppe Marco Tina, Antonio Gagliano and Stefano Aneli, 'Electrical and Thermal Performances of Bi-fluid PV Thermal Collectors', Article, National School of Applied Sciences, Mohmed First Univer, Published 15 March 2021

[7]. KHELIFA Abdelkrim,' Contribution à la conception et modélisation d'un capteur solaire hybride photovoltaïque thermique PVT', thèse de doctorat, Université Hadj Lakhdar de Batna Département des sciences de la matière Faculté des sciences, 22/01/2017

[8]. GHELLAB Amel.' Modélisation et optimisation des capteurs solaires hybrides', Thèse de doctorat, Université des Frères Mentouri Constantine, 11/02 / 2018.

[9]. ZAZOUA Imad Eddine, BENLAFKIR Abdennacer.' Prédiction des performances d'un capteur hybride PVT à l'aide des réseaux de neurones artificiels, Mémoire de master, Université Mohamed Seddik Ben Yahia – Jijel, 2018.

[10]. HAYIBO Koami Soulemane.' Modélisation et simulation d'un capteur solaire hybride photovoltaïque thermique', Mémoire de master, Université de Ouaga I, 10/11/2016.

[11]. TABET Ismail.' Étude, Réalisation et simulation d'un capteur solaire', thèse de doctorat, Université des Frères Mentouri Constantine, 19 /01 /2016.

[12]. BEDDIAR Saloua - DJEDDI Samia,' Modélisation et simulation d'un système hybride photovoltaïque/thermique', Mémoire Master, Université Larbi Tébessi– Tébessa – Faculté des Sciences et de la Technologie Département de Génie électrique, 22 / 06 / 2021

[13]. Kamel SAHLAOUI, Salah Ben M,' Étude et Simulation d'un Capteur hybride Photovoltaïque Thermique à air', Article, Centre de Recherches et des Technologies de l'Energie. CRTEn. Laboratoire L.E.P.T. Bp95 Hammam-Life 2050; Tunisie, Conference Paper, October 2016

[14] LAHOUAZI F. Mise en œuvre d'une stratégie de commande neuro floue: Application à un pendule inversé. Mémoire de Master en Automatique, département Automatique, Université Mouloud Mammeri, Tizi-Ouzou. Soutenu le, 16/03/2011

[15]. FAIZA BELHACHAT,' Commande neuro-floue d'un hacheur MPPT', Mémoire Master, Ecole Nationale Polytechnique 10, Avenue Hassen Badi, El-Harrach, ALGER, Juin 2007

[16] ZAGHBA Layachi, 'Etude et Commande Adaptative par les Techniques Intelligentes Des Systèmes Non linéaires Application aux Systèmes Photovoltaïques', thèse de doctorat, Université Mohamed Khider – Biskra Faculté des Sciences et de la technologie, 27 / 11 / 2017

[17]. M Boubazine Yassine et M Bouchemlla Mohamed Badis. 'Étude d'un capteur solaire hybride photovoltaïque/thermique (PV/T) à air, Mémoire Master, Université de JIJEL, 2014/2015.

[18]. Ankit Gupta, Pawan Kumar, Rupendra Kumar Pachauri, Yogesh K. 'Analysis of Neural Network and Fuzzy Logic Based MPPT Techniques for Solar PV Systems', Chauhan Electrical Engineering Department, School of Engineering Gautam Buddha University Greater Noida, Uttar Pradesh (India) – 201308 Performance, 09 December 2015.

[19]. EL HAMEL L'ALLA GHODBANE SELMA,' Modélisation et simulation d'un système photovoltaïque optimisé par les algorithmes MPPT', Mémoire Master, Université Kasdi Merbah Ouargla, Faculté des Sciences Appliquées, Département de Génie Électrique, 2019/2020

[20]. Kamel Sahlaoui, Hatem Oueslati & Salah Ben Mabrouk,'Thermal and electrical performance evaluation of hybrid air PVT collector – numerical analysis and experimental s tudy', Article, Thermal and electrical performance evaluation of hybrid air PVT collector – numerical analysis and experimental study, International Journal of Sustainable Energy, (2021)

[21]. Amina Benhammou. "Optimisation d'un nouveau système de séchage solaire modulaire pour plantes aromatiques et médicinales," thesis, University Abou Beker Belkaid, Algeria, Feb. 2010.

[22]. DONA Victorien Bruno, MAXWELL Djaffard, et al, "Estimate of photovoltaic energy production during the sunniest month in Mahajanga", IJARIIE-ISSN(O)-2395-4396, Vol-5 Issue-4, pp. 92 - 103, 2019